Article

Cell Stem Cell

Skeletal Muscle Stem Cells from PSC-Derived Teratomas Have Functional Regenerative Capacity

Graphical Abstract

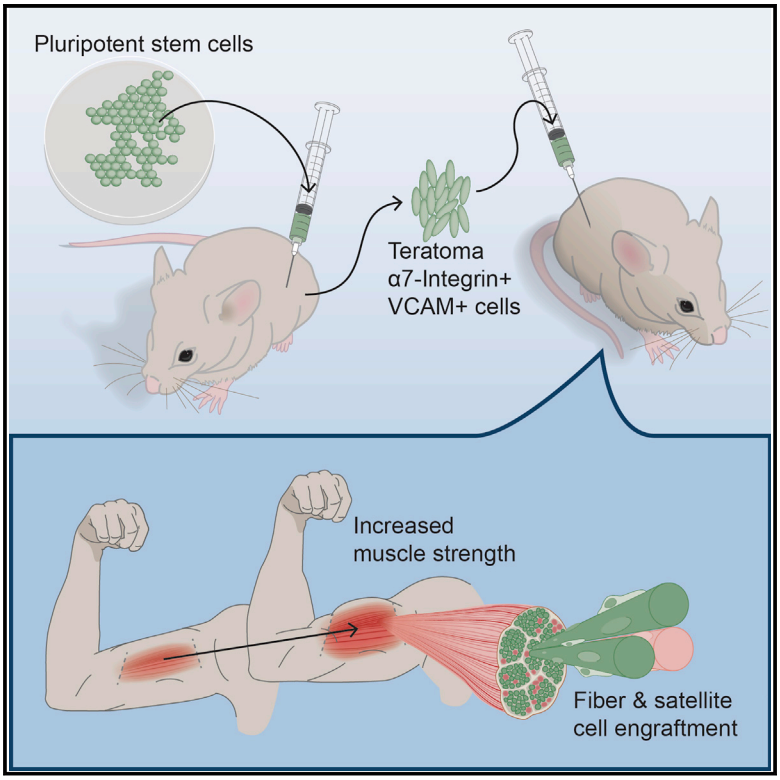

Authors

Sunny Sun-Kin Chan, Robert W. Arpke, Antonio Filareto, ..., Jacqueline S. Penaloza, Rita C.R. Perlingeiro, Michael Kyba

Correspondence

kyba@umn.edu

In Brief

Chan et al. show that functional skeletal muscle stem cells can be produced from mouse pluripotent stem cells without genetic modification through teratoma formation. As few as 40,000 teratoma-derived cells can regenerate 80% of total muscle volume, improve force generation, and mature into functional muscle stem cells *in vivo*.

Highlights

- Teratomas are rich in α7-Integrin+ VCAM-1+ myogenic progenitors
- 40,000 teratoma-derived α7+ VCAM+ cells reconstitute 80% of TA muscle fiber volume
- New fibers generate force and ameliorate dystrophin-related force deficiency
- Teratoma-derived myogenic progenitors mature into PAX7+ muscle stem cells *in vivo*

Chan et al., 2018, Cell Stem Cell *23*, 74–85
July 5, 2018
https://doi.org/10.1016/j.stem.2018.06.010

CellPress

CellPress

Cell Stem Cell
Article

Skeletal Muscle Stem Cells from PSC-Derived Teratomas Have Functional Regenerative Capacity

Sunny Sun-Kin Chan,[1,2,4] Robert W. Arpke,[1,2,4] Antonio Filareto,[1,3] Ning Xie,[1,2] Matthew P. Pappas,[1] Jacqueline S. Penaloza,[1,2] Rita C.R. Perlingeiro,[1,3] and Michael Kyba[1,2,5,*]
[1]Lillehei Heart Institute, University of Minnesota, Minneapolis, MN 55455, USA
[2]Department of Pediatrics, University of Minnesota, Minneapolis, MN 55455, USA
[3]Department of Medicine, University of Minnesota, Minneapolis, MN 55455, USA
[4]These authors contributed equally
[5]Lead Contact
*Correspondence: kyba@umn.edu
https://doi.org/10.1016/j.stem.2018.06.010

SUMMARY

Derivation of functional skeletal muscle stem cells from pluripotent cells without genetic modification has proven elusive. Here we show that teratomas formed in adult skeletal muscle differentiate *in vivo* to produce large numbers of α7-Integrin+ VCAM-1+ myogenic progenitors. When FACS-purified and transplanted into diseased muscles, mouse teratoma-derived myogenic progenitors demonstrate very high engraftment potential. As few as 40,000 cells can reconstitute ~80% of the *tibialis anterior* muscle volume. Newly generated fibers are innervated, express adult myosins, and ameliorate dystrophy-related force deficit and fatigability. Teratoma-derived myogenic progenitors also contribute quiescent PAX7+ muscle stem cells, enabling long-term maintenance of regenerated muscle and allowing muscle regeneration in response to subsequent injuries. Transcriptional profiling reveals that teratoma-derived myogenic progenitors undergo embryonic-to-adult maturation when they contribute to the stem cell compartment of regenerated muscle. Thus, teratomas are a rich and accessible source of potent transplantable skeletal muscle stem cells.

INTRODUCTION

PAX7+ satellite cells are responsible for muscle maintenance and regeneration after injury throughout life (Günther et al., 2013; Seale et al., 2000; von Maltzahn et al., 2013). They are rare, making up 1%–2% of the mononuclear fraction of skeletal muscle (Bosnakovski et al., 2008), itself a small fraction of total muscle mass, which is comprised mainly of multinucleated muscle fibers. Satellite cells associate intimately with fibers, residing under the fiber basal lamina (Mauro, 1961), and cannot be isolated without destroying muscle tissue; therefore, only relatively small biopsies are feasible for human transplantation. Although freshly isolated satellite cells have tremendous regenerative potential (Arpke et al., 2013; Collins et al., 2005; Hall et al., 2010; Sacco et al., 2008), it is insufficient to enable a meaningful therapy from a small biopsy. In culture, satellite cells activate and convert into myoblasts, whose transplantation potential is limited (Gussoni et al., 1992; Mendell et al., 1995; Montarras et al., 2005; Sacco et al., 2008). Embryonic stem cells (ESCs) and induced pluripotent stem cells (iPSCs) have unlimited expansion potential, theoretically enabling large numbers of derivative cells for transplantation; however, skeletal myogenesis does not arise spontaneously from pluripotent cells *in vitro*, and although progress is being made (Chal et al., 2015; Shelton et al., 2014), cells capable of generating functional force-producing muscle after transplantation have only been derived through genetic modification of pluripotent cells to overexpress PAX3 (Darabi et al., 2008; Filareto et al., 2013) or PAX7 (Darabi et al., 2012).

The skeletal muscle lineage derives from a complex morphogenetic pathway, somitogenesis, involving precisely timed mesenchymal condensation, patterning by neural tube and notochord, and delamination of myogenic progenitors. *In vitro* methods have not yet approached this complexity of morphogenesis; however, teratomas derived from pluripotent stem cells implanted into live hosts are capable of producing highly complex mature tissues: hair follicles, glands, and other structures. Also, it has been reported that transplantable hematopoietic stem cells arise within teratomas in both the mouse (Suzuki et al., 2013), and the human system (Amabile et al., 2013). We therefore investigated teratomas for signs of skeletal myogenic progenitor formation, evaluated the nature of these progenitors, and investigated their *in vivo* muscle formation, force generation, and stem cell compartment engraftment potential.

RESULTS

α7-Integrin+ VCAM-1+ Teratoma Cells Are Skeletal Muscle Progenitors

To maximize access of teratoma-derived cells to a promyogenic environment, we implanted EGFP+ murine ESCs (E14-EGFP ESCs) (Ismailoglu et al., 2008) into injured, irradiated *tibialis anterior* (TA) muscles of NSG-mdx^{4Cv} mice. These animals are both immune- and dystrophin-deficient and, therefore,

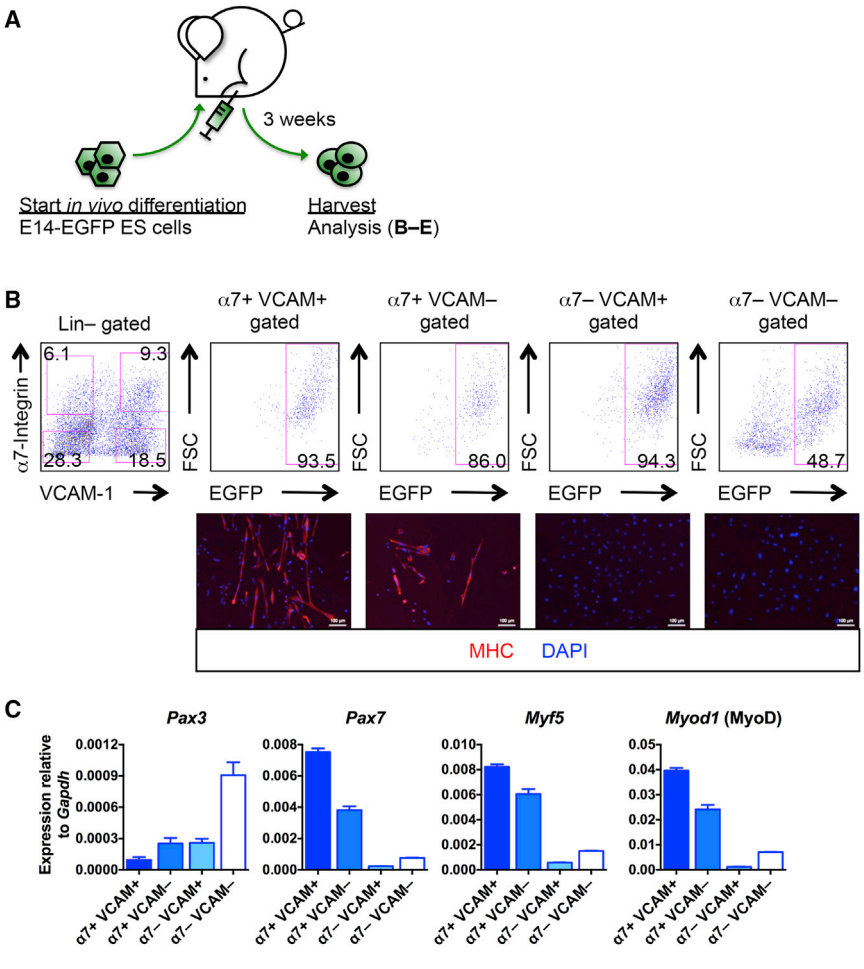

Figure 1. Myogenic Progenitors Are Found in Teratomas

(A) Schematic of generating myogenic progenitors from EGFP-labeled E14 (E14-EGFP) ESCs *in vivo*.

(B) E14-EGFP ESC-derived myogenic progenitors. FACS profiling (top row) of 3-week-old teratomas revealed the presence of α7+ VCAM+ and α7+ VCAM– putative myogenic progenitors. Immunostaining (bottom row) confirmed their myogenic identity (MHC+) (n = 6 biological replicates). The other 2 fractions, α7– VCAM+ and α7– VCAM–, had minimal myogenic potential (n = 4 biological replicates). Scale bars represent 100 μm.

(C) qRT-PCR for markers for muscle stem cells (*Pax3* and *Pax7*), activated myogenic progenitor cells (*Myf5*), and myogenically committed cells (*Myod1*) (n = 6 from 2 biological replicates). Note that *Pax3* is also a marker of neuroectoderm derivatives.

(D) Clonal analysis showing that single α7+ VCAM+ or α7+ VCAM– cells were capable of forming MHC+ myogenic colonies with differentiated myoblasts and multi-nucleated myotubes. Ratios indicate the number of colonies developed per number of single cells seeded (n = 5 biological replicates). The scale bar represents 100 μm.

(E) Cytospins of α7+ VCAM+ cells showing that 30% expressed PAX7+, a muscle stem cell transcription factor (n = 4 biological replicates). The scale bar represents 100 μm.

α7, α7-integrin. VCAM, VCAM-1. ES cells, embryonic stem cells. Lin, lineage cocktail comprising antibodies against CD45 (hematopoietic) and CD31 (endothelial). MHC, myosin heavy chain. Mean ± SEM is shown in (C). See also Figure S1.

allow not only facile engraftment but unequivocal assignment of a donor identity (DYSTROPHIN+) to regenerated muscle tissue (Arpke et al., 2013). Prior to implantation, hindlimbs were irradiated to impair host satellite cells, and TA muscles were injected with cardiotoxin to kill host fibers and to stimulate myogenesis. Using flow cytometry on 3-week teratomas (Figure 1A), we evaluated the population of cells negative for the hematopoietic and endothelial markers CD45 and CD31 (Lin–) with antibodies to the satellite cell markers α7-integrin and vascular cell adhesion molecule-1 (VCAM-1) (hereafter referred to as α7 and VCAM, respectively) (Blanco-Bose et al., 2001; Chan et al., 2013; Fukada et al., 2007; Jesse et al., 1998; Seale et al., 2004). The α7+ VCAM+ population was abundant, forming about 10% of the total Lin– fraction, and the majority of α7+ VCAM+ cells were also EGFP+; i.e., donor-derived (Figures 1B and S1A). Teratomas also contained host-derived hematopoietic, endothelial, and other cells, demonstrating that the teratoma vigorously interacts with its host, with potential effects on differentiation (Figure S1B). We found minimal expression of other satellite cell markers on Lin– cells, such as CD34 or CXCR4 (Figure S1C). Although α7+ VCAM+ cells were prominent at 3 weeks and beyond, their emergence could first be detected 2 weeks post-ESC implant (Figures S1D and S1E).

We sorted cells based on α7 and VCAM expression and found that the α7+ fractions contained mRNA for myogenic transcription factors (Figure 1C). Interestingly, although both α7+ fractions express the embryonic myogenic factor *Pax3*, its expression is more abundant in the double-negative fraction, indicating that most *Pax3* expression in teratomas probably comes from neuroectodermal cells. Both α7+ fractions generated differentiated myotubes *in vitro*; however, at a single-cell level, myogenic clones were more frequent in the α7+ VCAM+ population (Figure 1D). We evaluated PAX7 protein expression by immunostaining cytospins of Lin– α7+ VCAM+ cells. This

revealed the population to be heterogeneous, with about 30% of cells expressing PAX7 (Figure 1E). To determine the proliferative capacity of these cells, we subjected them to long-term *ex vivo* culture. We found that teratoma-derived α7+ VCAM+ cells could be exponentially expanded up to at least 12 passages, with the expanded cells retaining robust myogenic potential (Figure S1F). This is notable because myoblasts from adults are reported to lose myogenic potential with extended passage (Penton et al., 2016).

The teratomas described above were formed in muscle that was irradiated and cardiotoxin-injured to enhance myogenesis and to minimize host contribution to the α7+ VCAM+ compartment. To evaluate the necessity of irradiation and injury, we formed teratomas in hosts pretreated in various ways and evaluated the development of myogenic progenitors (Figures S1G and S1H). EGFP+ α7+ VCAM+ cells were found in all scenarios, and they had comparable potential in forming myotubes *in vitro* and fibers after transplantation (see below). Nevertheless, the irradiated and injured hosts showed much greater enrichment of EGFP+ cells within the α7+ VCAM+ fraction, and, thus, teratomas were formed in irradiated, injured hosts for all following experiments.

Primary Myogenic Cells from Teratomas Have Extremely High *In Vivo* Regenerative Potential

To test the *in vivo* regenerative potential of these α7+ VCAM+ cells, we performed transplants of 40,000 EGFP+ Lin– α7+ VCAM+ cells into TA muscles of new NSG-mdx^{4Cv} recipients (Figure 2A). Prior studies transplanting myoblasts (Partridge et al., 1989) or PAX3 or PAX7-modified pluripotent cells (Darabi et al., 2008) have used one or more orders of magnitude more cells. We began with this relatively low number in order to transplant a number of PAX7+ cells close to the number of endogenous PAX7+ cells in a single TA muscle (Brack et al., 2005). One month post-transplant, we observed muscle regeneration on a scale that significantly surpassed previous reports. The engraftment of DYSTROPHIN+ fibers was pervasive (Figures 2B and 2C). One month post-transplant, this accounted for approximately two-thirds of the TA muscle, and at 3 months about 80% of the total muscle cross-sectional area (Figures 2C and 2D). These newly formed DYSTROPHIN+ fibers were of varied phenotypes, consisting of both slow (myosin heavy chain I [MHC-I]) and fast (MHC-IIa and MHC-IIb) twitch fibers (Figure 2E; Figure S2A).

Because the recipient mice were irradiated to prevent the contribution of endogenous cells to regeneration, we infer that the regenerated DYSTROPHIN+ fibers predominately derived from donor cells. Nevertheless, we wished to rigorously evaluate the donor:host ratio using a direct approach. Because the NSG-mdx^{4Cv} recipient mice are homozygous for a SNP in the *Prkdc* gene (the severe combined immunodeficiency [SCID] mutation), we amplified this region from total genomic DNA from transplanted TA muscles and evaluated the frequency of donor versus host DNA sequence (Figure 2F). This revealed the average donor contribution to be over 50% of the total genomic DNA content of the transplanted TA muscle. It is notable that the TA muscle contains many host-derived non-myogenic cell types, such as fibroblasts, endothelial cells, and hematopoietic cells, all of which contribute to the host component of this measurement, so this value is consistent with the donor fibers being almost exclusively derived from donor nuclei.

To ensure that differentiation via teratoma had not led to undesirable changes in the cells being transplanted, we evaluated karyotypes of α7+ VCAM+ cells. This revealed that teratoma-derived cells did not acquire any numerical and structural chromosomal abnormality, and they retained a normal karyotype after serial passages (Figure S2B). We further evaluated the status of the regenerated muscle for signs of abnormally maintained proliferation and differentiation. Embryonic MHC, a marker of recently generated fibers, was present in only a negligible portion of DYSTROPHIN+ fibers 1 month post-transplant, and its expression was completely absent after 3 months (Figure S2C), indicating that the newly formed fibers were maturing and that new fibers were not being generated indefinitely. To determine whether an abnormal population of proliferating mononuclear cells was present, we administered a 3-day pulse of 5-ethynyl-2′-deoxyuridine (EdU) 3 months post-transplant and harvested the TA muscles 5 weeks later. We did not observe any EdU incorporation or any embryonic MHC positivity in DYSTROPHIN+ fibers (Figure S2D), indicating that the engrafted cells became quiescent over time. Neither did we observe any secondary teratomas forming after transplantation in well over 100 transplantations of teratoma-derived α7+ VCAM+ cells, 12 of which were evaluated at 1 year. Taken together, these data suggest that teratoma formation per se does not induce carcinogenicity.

To test the effect of irradiation, which eliminates host competition, and cardiotoxin injury, which initiates widespread regeneration, we tested transplants of teratoma-derived α7+ VCAM+ cells without irradiation and injury. Although engraftment was lower in these cases, α7+ VCAM+ cells were capable of forming large numbers of new fibers in irradiation-only muscles, injury-only muscles, and also in non-irradiated uninjured muscles (Figure S2E).

To determine whether the newly formed muscle tissue was functional, we measured its force generation capability (Figure 2G). The maximal tetanic force generated by the α7+ VCAM+ cell-regenerated muscles was approximately 3 times greater than that of the sham contralateral controls, indicating that the new muscle fibers are functional; i.e., capable of generating force when stimulated. The engrafted muscles also showed greatly increased specific force (maximal force normalized to the size of the muscle). This improved quality of force metric reflects the fact that the newly engrafted muscle is DYSTROPHIN+ and, thus, less diseased, whereas the disease process was ongoing in the contralateral leg and possibly amplified because of the impairment of host satellite cells by the irradiation. In addition, the time to fatigue after repetitive contractions was much increased in the cell-transplanted TA muscles versus contralateral controls, further reflecting the DYSTROPHIN+ nature of the newly formed muscle.

To further demonstrate the functionality of these newly formed fibers, we tested whether they were innervated and, thereby, integrated into the recipient environment. Staining with the presynaptic marker α-bungarotoxin revealed its close proximity to DYSTROPHIN+ fibers, suggesting the presence of neuromuscular junctions in these fibers (Figure 2H).

The substantial muscle-regenerative potential of these α7+ VCAM+ myogenic cells encouraged a direct comparison with

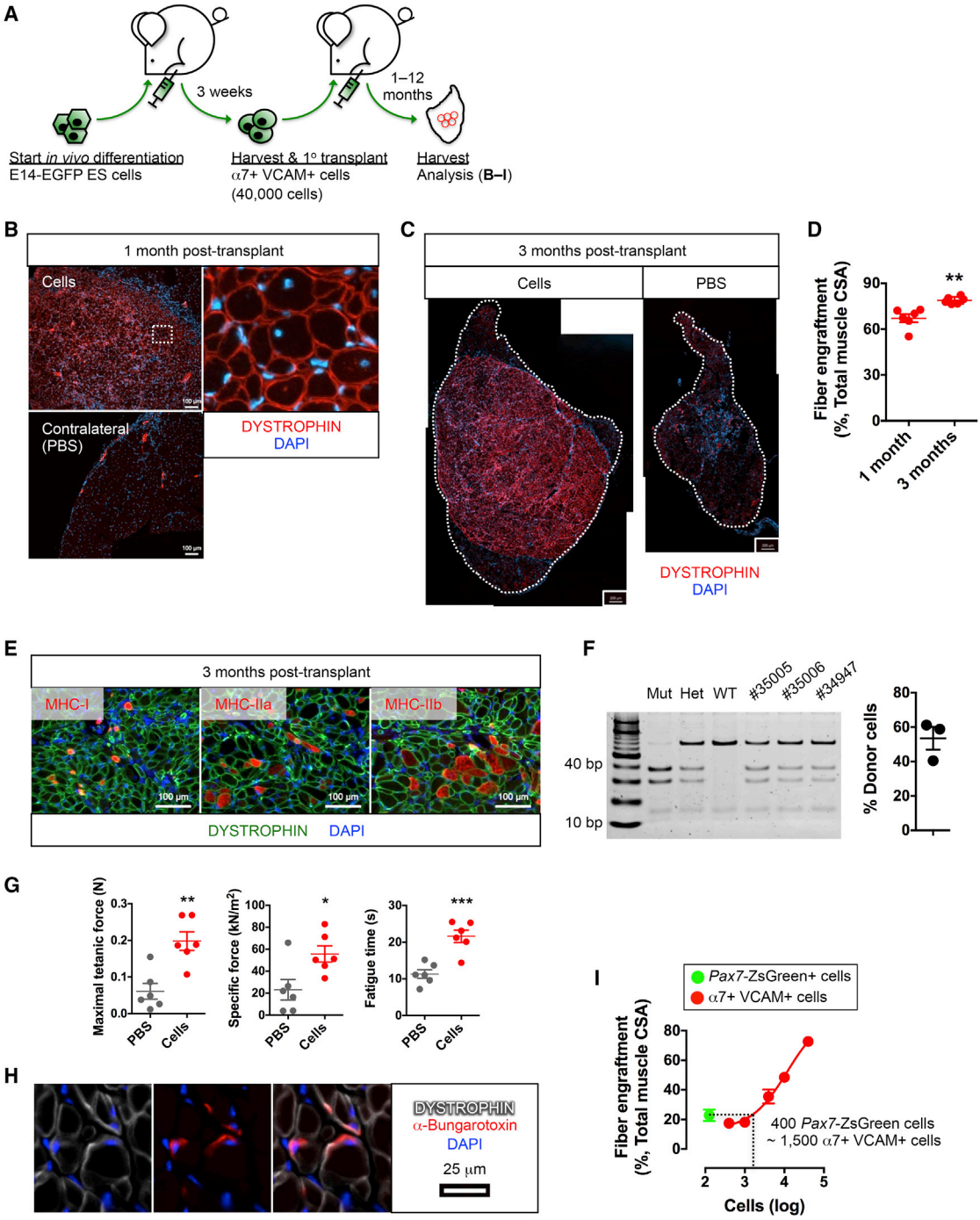

Figure 2. ESC-Derived Myogenic Progenitors Reconstitute Functional Fibers

(A) Schematic of functional evaluation of E14-EGFP ESC-derived α7+ VCAM+ myogenic progenitors.

(B–F) ESC-derived α7+ VCAM+ myogenic progenitors engrafted and differentiated into functional muscle fibers.

(B) α7+ VCAM+ myogenic progenitors engrafted and differentiated into DYSTROPHIN+ muscle fibers (top left) (n = 18 biological replicates). Areas indicated by the white dotted rectangle are magnified to show individual fibers (top right). Minimal DYSTROPHIN+ revertant fibers were observed in the contralateral muscle with PBS injection (bottom left). Scale bars represent 100 μm.

(C) Engraftment (DYSTROPHIN+ fibers) at 3 months, comparing injected (left) with contralateral PBS-injected (right) (n = 6 biological replicates). The whole TA muscle is outlined. Note that several separate images were stitched together to show the whole TA section. Scale bars represent 200 μm.

(D) Quantitation of fiber engraftment (DYSTROPHIN+ fibers) at 1 month and 3 months (n = 6 biological replicates). **$p < 0.01$ versus 1 month.

(E) Engrafted DYSTROPHIN+ muscle fibers consist of slow-twitch (MHC-I) and fast-twitch (MHC-IIa and MHC-IIb) fibers (n = 6 biological replicates). Scale bars represent 100 μm.

(legend continued on next page)

bona fide satellite cells. We used the *Pax7*-ZsGreen reporter mouse (Bosnakovski et al., 2008) to isolate adult satellite cells by fluorescence-activated cell sorting (FACS) and compared the fiber formation of these with the fiber formation of various numbers of teratoma-derived α7+ VCAM+ cells, establishing the dose-response relationship for fiber engraftment (Figures 2I and S2F). Remarkably, 1,500 teratoma-derived α7+ VCAM+ cells are functionally equivalent to 400 freshly isolated *Pax7*-ZsGreen+ cells.

Previously published data with transplantation from *in vitro*-differentiated pluripotent cells have shown only small clusters of, at most, 200 fibers. Using the same injury and irradiation protocol in the same host strain, we directly compared teratoma differentiation to *in vitro* differentiation. We adopted a monolayer differentiation protocol (Chal et al., 2015) and detected α7+ VCAM+ cells with myogenic potential after 4 weeks of culture (Figure S2G). We subsequently transplanted 40,000 α7+ VCAM+ sorted cells and harvested the transplanted TA muscles 3 months later. This comparison was consistent with the published data and showed that cells generated via *in vitro* differentiation give much poorer engraftment than cells derived via teratoma formation (Figure S2G).

To demonstrate that the development of myogenic progenitors was not restricted to the 129P2/Ola background from which our E14 ESCs derive, we repeated the experiments using another ESC line with a C57BL/6N background (C57BL/6N-PRX-B6N #1). Similarly, α7+ VCAM+ cells were found in 3-week-old C57BL/6N teratomas and, upon transplantation into NSG-mdx^{4Cv} recipients, formed DYSTROPHIN+ muscle fibers (Figure S2H).

A Subpopulation of Cells Engrafts as Functional Muscle Stem Cells

Long-term maintenance of new skeletal muscle is ultimately dependent on the ability of the transplanted cells to contribute to the skeletal muscle stem cell pool. Immunostaining revealed PAX7+ EGFP+ cells associated with DYSTROPHIN+ fibers under the basal lamina (Figure 3A–3C). We did not observe teratoma-derived cells in the skeletal muscle interstitium or any circulating teratoma-derived myogenic cells in the peripheral blood by FACS (data not shown). We then analyzed a cohort of recipients for contribution to the stem cell compartment by digesting the transplanted TA muscles into individual cells and testing for donor-derived (EGFP+) cells in the mononuclear fraction. Transplanted muscles had an abundant α7+ VCAM+ population within the Lin– fraction, and the great majority of these cells were donor derived; i.e., EGFP+ (Figure 3D). Re-isolated donor-derived cells differentiated into multinucleated myotubes *in vitro*, indicating that they are indeed myogenic progenitors (Figure 3E).

To rigorously characterize the regenerative potential of the engrafted mononuclear cell population, we tested the regenerated muscle by re-injury (Figure 3F). Three months after performing primary transplants of teratoma-derived α7+ VCAM+ cells into both TAs, we re-injured one of the muscles and administered EdU for 3 days. TA muscles were then harvested 5 days or 5 weeks after re-injury. In the 5-day post-injury cohort, EdU+ embryonic MHC+ cells were readily observed, indicating robust regeneration after injury (Figure 3G). In the 5-week post-injury cohort, EdU+ DYSTROPHIN+ fibers were now found in the re-injured TA muscle, whereas the DYSTROPHIN+ muscle fibers of the contralateral TA were EdU–. This demonstrates that the engrafted, quiescent, mononuclear fraction is capable of proliferating in response to re-injury and of generating a secondary regenerate (Figure 3H).

We next performed a series of studies using iPSCs we generated from the *Pax7*-ZsGreen reporter mouse, in which quiescent satellite cells express the ZsGreen reporter (Bosnakovski et al., 2008). In the initial teratomas, we found, surprisingly, that the *Pax7*-ZsGreen reporter was not expressed in a significant fraction of the α7+ VCAM+ population (Figures 4A and 4B). Nevertheless, like their ESC-derived cognates, the iPSC-derived α7+ VCAM+ cells could differentiate into MHC-expressing multinucleated myotubes *in vitro*, both in bulk and clonally (Figures 4C and 4D). When transplanted into NSG-mdx^{4Cv} recipients, the iPSC-derived α7+ VCAM+ cells formed abundant myofibers (Figure 4E). Multiple independent *Pax7*-ZsGreen iPSC clones gave similar results (Figure S3A). Most importantly, in these transplanted muscles, we now found a large population of *Pax7*-ZsGreen+ α7+ VCAM+ cells (Figures 4F and S3B); thus, although the *Pax7*-ZsGreen reporter is not expressed in the α7+ VCAM+ cells of the teratoma, it becomes expressed in the α7+ VCAM+ cells of the newly regenerated muscle. To confirm that the donor-derived mononuclear *Pax7*-ZsGreen cells in the regenerated muscle were indeed skeletal muscle stem cells, we isolated them and tested their myogenic differentiation potential both *in vitro* by colony assays and *in vivo* by secondary transplantation. They produced MHC+ DYSTROPHIN+ myotubes *in vitro* (Figure 4G) and myofibers in NSG-mdx^{4Cv} hosts (Figure 4H). This demonstrates that, in addition to regenerating muscle fibers and rebuilding damaged muscle, teratoma-derived myogenic progenitors populate this new muscle with mature PAX7+ α7+ VCAM+ definitive skeletal muscle stem cells.

Notably, the *Pax7*-ZsGreen reporter was expressed in many more α7+ VCAM+ cells in regenerated muscle than in teratomas, suggesting maturation from an embryonic progenitor (Bober et al., 1994; Goulding et al., 1994) into a PAX7+ quiescent adult satellite cell (Kuang et al., 2006) only after removal from the teratoma and transplantation into adult muscle.

(F) Contribution of donor nuclei in transplanted muscle. SCID PCR of total genomic DNA from transplanted muscles (left) and quantification (right). The first 3 control lanes represent the following: Mut, *Prkdc*$^{SCID/SCID}$; Het, *Prkdc*$^{+/SCID}$; WT: *Prkdc*$^{+/+}$. The 3 right lanes represent transplanted muscles.

(G) *Ex vivo* physiological assessment revealed functional improvement 3 months after α7+ VCAM+ cell transplantation (n = 6 biological replicates). *p < 0.05, **p < 0.01, ***p < 0.001 versus PBS (vehicle).

(H) Cross-section showing pre-synaptic staining with α-bungarotoxin in DYSTROPHIN+ fibers (n = 3 biological replicates). The scale bar represents 25 μm.

(I) Comparison of *Pax7*-ZsGreen satellite cells and α7+ VCAM+ teratoma cells. 400 *Pax7*-ZsGreen cells are equivalent to 1,500 α7+ VCAM+ cells for fiber engraftment (n = 4–5 biological replicates). The raw data for generating the dose-response relationship are shown in Figure S2F.

α7, α7-integrin; VCAM, VCAM-1; CSA, cross-sectional area; ESCs, embryonic stem cells; Lin, lineage cocktail comprising antibodies against CD45 (hematopoietic) and CD31 (endothelial); MHC, myosin heavy chain. Mean ± SEM is shown in (D), (F), (G), and (I). See also Figure S2.

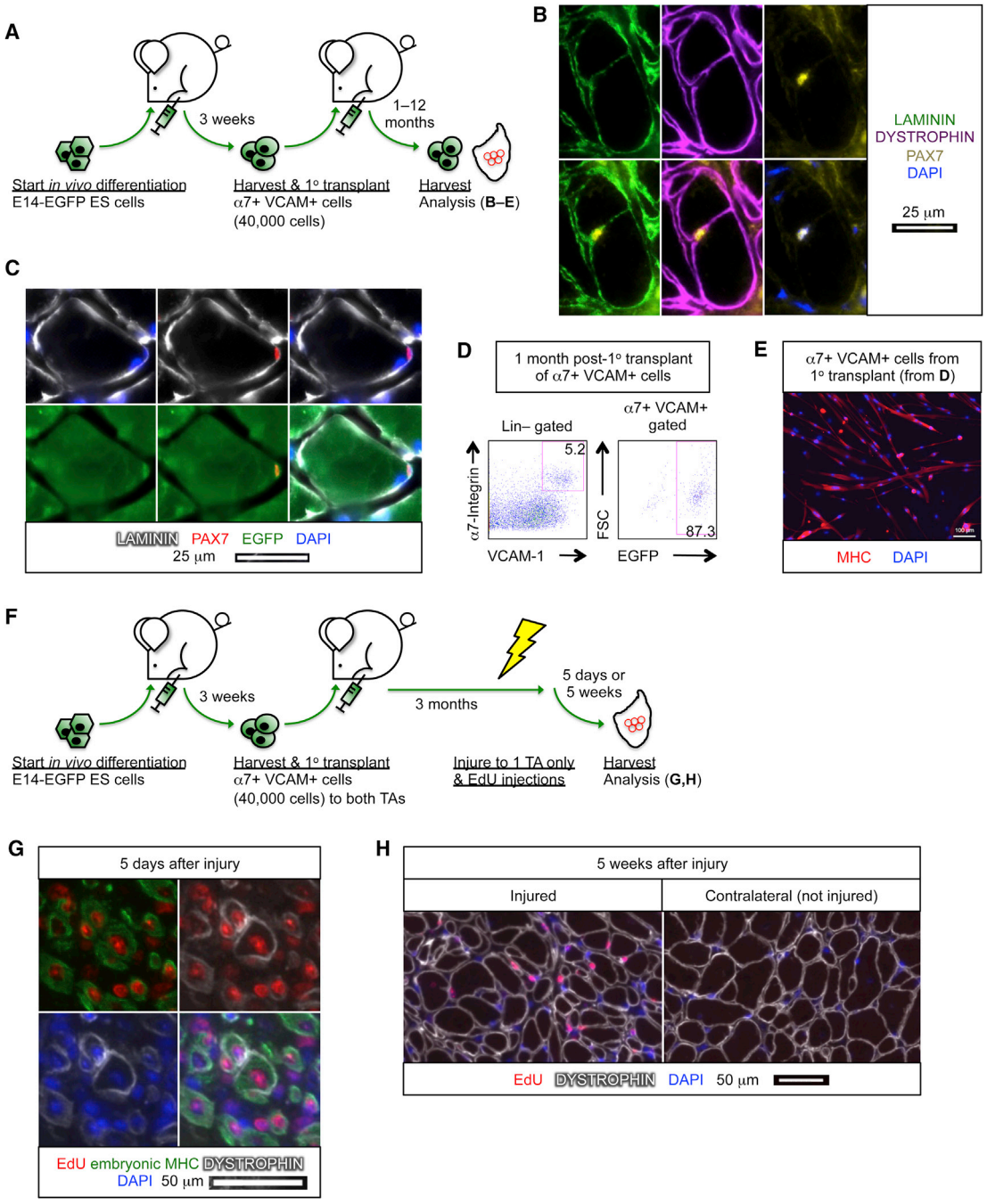

Figure 3. ESC-Derived Myogenic Progenitors Reconstitute the Muscle Stem Cell Compartment

(A) Schematic of evaluating the contribution of E14-EGFP ESC-derived α7+ VCAM+ myogenic progenitors in the muscle stem cell compartment.

(B) PAX7+ cell associated with a DYSTROPHIN+ fiber under the basal lamina (n = 6 biological replicates). The scale bar represents 25 μm.

(C) Donor derived PAX7+ EGFP+ muscle stem cell under the basal lamina (n = 6 biological replicates). The scale bar represents 25 μm.

(D) FACS analysis of transplanted muscles revealed that the majority of α7+ VCAM+ muscle stem cells are also EGFP+; i.e., donor-derived (n = 7 biological replicates).

(E) Re-harvested α7+ VCAM+ EGFP+ cells (from D) differentiated into multi-nucleated MHC+ myotubes upon culture (n = 7 biological replicates). The scale bar represents 100 μm.

(F) Schematic of evaluating the regenerative potency of transplanted E14-EGFP ESC-derived α7+ VCAM+ myogenic progenitors upon subsequent injury.

(G and H) Transplanted α7+ VCAM+ cells regenerate upon subsequent injury. α7+ VCAM+ cells were transplanted into both left and right TA muscles, and, 3 months later, only the left TA muscles were re-injured. EdU was administered 2–4 days after re-injury. Muscles were then harvested (G) 5 days or (H) 5 weeks after injury.

(legend continued on next page)

α7-Integrin+ VCAM-1+ Teratoma Cells Mature after Transplantation

To better understand the nature of teratoma-derived α7+ VCAM+ myogenic progenitors before and after transplantation, we performed RNA sequencing (RNA-seq) on α7+ VCAM+ cells isolated from teratomas, their mononuclear progeny after transplantation and repopulation of the new muscle satellite cell compartment, and for comparison of α7+ VCAM+ myogenic progenitors of isogenic (129P2/OlaHsd) E14.5 embryos and hindlimbs of 8-week-old 129P2 mice (*Teratoma*, *Transplant*, *Embryo*, and *Adult*, respectively; Figure 5A). It is important to emphasize that all four populations are very similar in nature; they were all highly purified on α7+ and VCAM+, and they are all myogenic. To illustrate this point, we performed principal-component analysis (PCA), including non-myogenic cell types such as undifferentiated ESCs and hematopoietic progenitors (datasets from ENCODE; https://www.encodeproject.org/), and, indeed, all 4 α7+ VCAM+ populations cluster very close together (Figure 5B; Figure S4A). Hierarchical clustering of differential genes revealed that the transcriptome of the teratoma α7+ VCAM+ population was most closely related to that of the embryonic α7+ VCAM+ population, whereas the α7+ VCAM+ cells in transplanted regenerated muscle were most closely related to the adult satellite cell population (Figure 5C; Tables S1 and S2). Indeed, gene ontology (GO) analysis showed similar enrichment between the *Teratoma-Transplant* comparison and the *Embryo-Adult* comparison (Figure 5D). Notably, genes that are upregulated in both the *Teratoma* and *Embryo* samples were related to cell division and DNA replication, reminiscent of an embryonic myoblast signature of rapid growth and proliferation (Figures 5E and 5F). On the other hand, both *Transplant* and *Adult* α7+ VCAM+ cells are enriched for genes pertaining to extracellular matrix regulation, likely involved in satellite cell niche signaling and quiescence (Figures 5E and 5F).

To gain insight into why teratoma-derived skeletal myogenic progenitors have such high engraftment efficiency, we performed GO analysis on the *Teratoma-Embryo* comparison and the *Transplant-Adult* comparison (Figures S4B and S4C; Tables S3 and S4). Interestingly, the T*eratoma* sample is enriched for genes related to immune response and cell migration, suggesting that teratoma α7+ VCAM+ cells may have an enhanced ability to evade the host's remaining immune system (the NSG mice still have functional neutrophils and monocytes) and to migrate to distant areas of the muscle, away from the site of injection. In contrast, compared with the *Adult* sample, genes enriched in the *Transplant* sample are related to muscle development, perhaps indicating that maturation is an ongoing process. Taken together, our data support that teratoma-derived α7+ VCAM+ cells are embryonic in nature but, after transplantation into adult muscle, undergo an *in vivo* maturation into quiescent muscle stem cells.

DISCUSSION

Here we describe a simple and efficient method for generating skeletal myogenic progenitors from pluripotent stem cells. Via teratoma formation within the TA muscle, α7+ VCAM+ cells arise robustly within 3 weeks, and, more importantly, on a per-cell basis, these cells have remarkable *in vivo* regenerative potential, developing into muscle fibers with similar efficiency to that of freshly isolated satellite cells and capable of regenerating 80% or more of the TA muscle fibers and providing over 50% of the total genomic DNA of the post-transplant TA muscle. With conventional tissue culture, it has proven difficult to efficiently derive myogenic progenitors from pluripotent stem cells, and, to date, the only functional force-generating repopulating cells reported have been derived through genetic modification to overexpress PAX3 or PAX7 (Darabi et al., 2008, 2012).

Another somatic stem cell type that has proven difficult to derive from unmodified pluripotent stem cells is the hematopoietic stem cell (HSC). Although pluripotent cells differentiate efficiently into blood progenitors, these progenitors do not have the capacity to engraft long-term unless genetically modified with self-renewal factors (Kyba et al., 2002; Perlingeiro et al., 2001). It was recently reported that transplantable blood progenitors can be identified within teratomas (Suzuki et al., 2013) although, in some cases, with low engraftment potential (Amabile et al., 2013). It is remarkable that the skeletal muscle stem cells isolated from teratomas function equivalently to, if not better than, their definitive adult cognates in transplantation assays. When diluted to determine their fiber generation potential on a per-cell basis, they showed about 30% of the activity of freshly isolated satellite cells; however, this is about four orders of magnitude higher than other wild-type non-satellite cell muscle-regenerative cells described to date. Because we see no evidence of unwanted cell types 1 month post-transplant, the moderate difference in efficiency of engraftment of teratoma-derived α7+ VCAM+ cells is probably due to a cell-intrinsic difference in capacity; however, we cannot rule out that some fraction of the sorted cells fail to engraft. However, when comparing maximum engraftment potential at higher cell numbers, the fiber generation potential of satellite cells becomes non-linear earlier, so that satellite cells peak at restoring around one-third of the TA muscle (Arpke et al., 2013), whereas, with teratoma-derived α7+ VCAM+ cells, we find a mean of 70% of the muscle restored at 1 month and 80% at 3 months. This difference is probably due to the non-adult character of the teratoma-derived cells, a result supported by the gene expression analysis. The adult TA muscle, together with its stem cells, derives entirely from a small embryonic founder population; thus, the embryonic progenitors must have greater muscle generation potential than their adult derivatives. However, it is also worth considering that their embryonic character may endow them with altered migratory potential, allowing them to contribute to fibers over a greater range from the site of injection. In fact, GO term analysis from our RNA-seq data supported the notion that teratoma-derived cells might present different immune and migration responses, allowing superior regeneration potential. It is reasonable to assume that stem cells of other lineages could be

(G) The presence of EdU+ embryonic MHC+ fibers 5 days after re-injury indicates regeneration. EdU+ embryonic MHC+ fibers start to re-express DYSTROPHIN (n = 4 biological replicates). The scale bar represents 50 μm.

(H) EdU+ DYSTROPHIN+ fibers in the injured muscle 5 weeks post-injury. Note that, in the contralateral muscle that was not re-injured after the primary transplant, only EdU– DYSTROPHIN+ fibers were present (n = 4 biological replicates). The scale bar represents 50 μm.

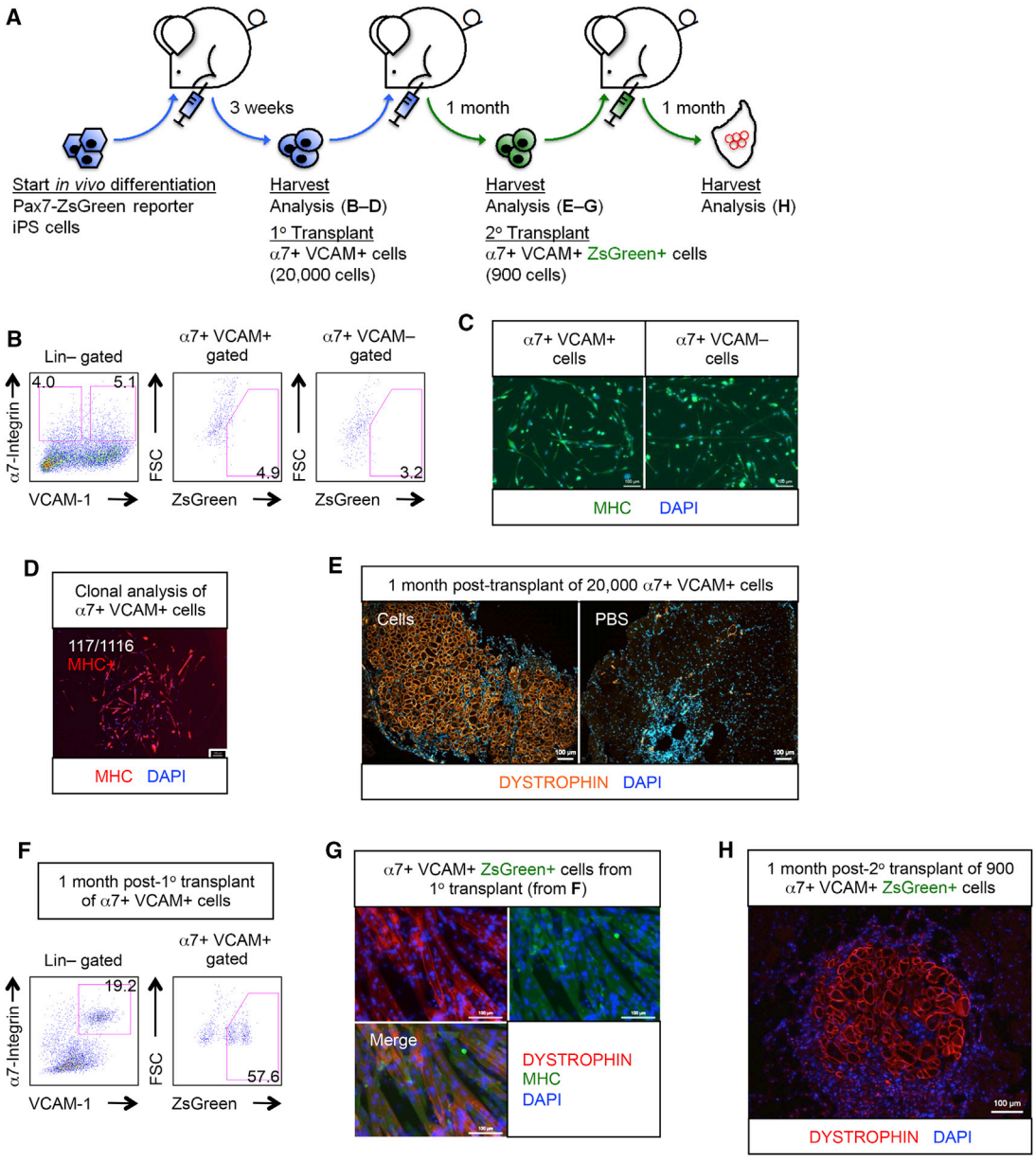

Figure 4. Myogenic Progenitors Derived from Teratomas Are Muscle Stem Cells

(A) Schematic of the transplantation experiment using *Pax7*-ZsGreen reporter iPSCs to test whether PAX7+ muscle stem cells are generated.

(B) α7+ VCAM+ and α7+ VCAM– myogenic progenitors were found in teratomas generated from *Pax7*-ZsGreen iPSCs, but ZsGreen was barely expressed in both fractions (n = 18 biological replicates).

(C) iPS teratoma-derived α7+ VCAM+ and α7+ VCAM– myogenic progenitors differentiated into MHC+ myogenic derivatives upon culture (n = 3 biological replicates). Scale bars represent 100 μm.

(D) Clonal analysis showing that single *Pax7*-ZsGreen reporter iPSC-derived α7+ VCAM+ cells were capable of forming MHC+ myogenic colonies with differentiated myoblasts and multi-nucleated myotubes (n = 12 biological replicates). Ratio indicates the number of colonies developed per number of single cells seeded. The scale bar represents 100 μm.

(E) iPSC teratoma-derived α7+ VCAM+ myogenic progenitors differentiated into muscle fibers upon transplantation (n = 12 biological replicates). Scale bars represent 100 μm.

(F) FACS analysis of transplanted muscles revealed that a significant fraction of the α7+ VCAM+ population is ZsGreen+; i.e., donor-derived muscle stem cells (n = 10 biological replicates). Compare this with (B).

(G) *In vitro* culture of α7+ VCAM+ ZsGreen+ muscle stem cells (from F) produced MHC+ DYSTROPHIN+ muscle fibers (n = 10 biological replicates). Scale bars represent 100 μm.

(H) α7+ VCAM+ ZsGreen+ muscle stem cells engrafted into the muscle fiber compartment upon transplantation (n = 3 biological replicates). The scale bar represents 100 μm.

See also Figure S3.

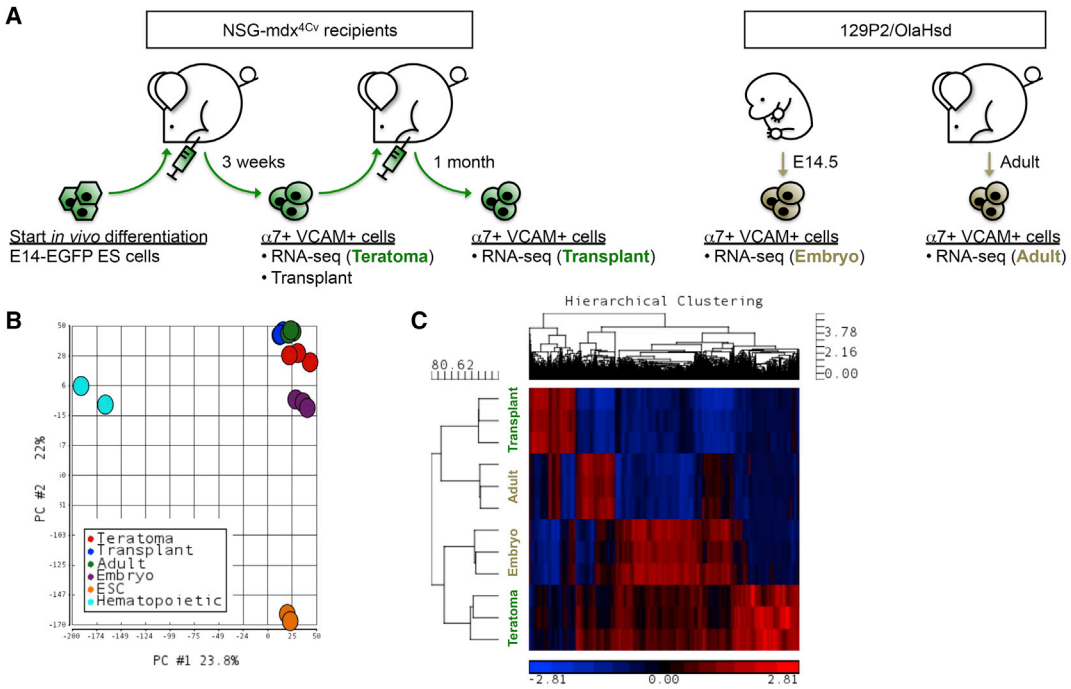

D

GO terms	Embryo up vs. Adult	Teratoma up vs. Transplant
Cell cycle	6.29×10^{-49}	8.52×10^{-29}
Cell division	1.93×10^{-36}	1.02×10^{-24}
DNA replication	9.25×10^{-16}	1.75×10^{-10}
Cell proliferation	7.45×10^{-3}	8.69×10^{-5}

GO terms	Adult up vs. Embryo	Transplant up vs. Teratoma
Negative regulation of cell proliferation	4.64×10^{-5}	6.18×10^{-3}
Extracellular matrix organization	2.53×10^{-3}	6.54×10^{-3}
Regulation of cell adhesion	4.23×10^{-3}	5.08×10^{-3}
Extracellular structure organization	9.74×10^{-3}	4.84×10^{-3}

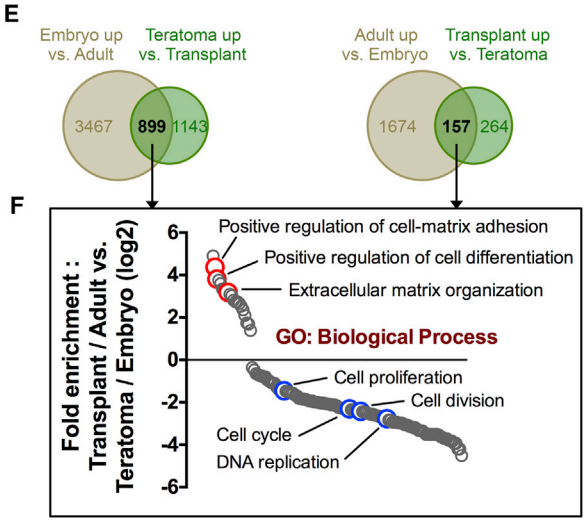

Figure 5. Teratoma-Derived Myogenic Cells Mature into Muscle Stem Cells after Transplantation

(A) Schematic of samples used for transcriptome analysis. α7+ VCAM+ myogenic cells were isolated from E14 ESC teratomas (*Teratoma*), transplanted TA muscles (*Transplant*), E14.5 embryos (*Embryo*), and 8-week-old adult hindlimbs (*Adult*) for RNA-seq (n = 3 biological replicates).

(B) Principal-component analysis (PCA). The transcriptomes of the 4 α7+ VCAM+ myogenic populations (*Teratoma*, *Transplant*, *Embryo*, and *Adult*) are very similar to each other in comparison with those of ESCs and hematopoietic progenitors. The ESCs and the hematopoietic progenitor RNA-seq datasets were obtained from ENCODE (https://www.encodeproject.org/).

(C) Hierarchical clustering of differentially expressed genes demonstrates a transcriptome similarity between *Transplant* myogenic cells and *Adult* satellite cells and between *Teratoma* cells and *Embryo* progenitors.

(D) Gene ontology (GO) biological process terms denoting genes enriched in the *Embryo-Adult* comparison (left column) and the *Teratoma-Transplant* comparison (right column). The p values of the GO terms are indicated.

(E) Venn diagrams showing differential genes commonly upregulated by *Teratoma* and *Embryo* progenitors and *Transplant* and *Adult* cells. The number of differential genes is indicated.

(F) Fold enrichment analysis of genes obtained from (E) based on GO biological processes.

See also Tables S1, S2, S3, and S4.

isolated with equal effectiveness from teratomas, and, given the results described here with muscle and above with blood, this idea merits further investigation.

The fact that cells are spontaneously differentiated within and isolated from teratomas raises the question of whether they might themselves be teratomagenic. However, unlike spontaneous teratomas in adults, those from pluripotent cells are not carcinogenic; it is only the pluripotent status of their founder cells that presents a risk of overgrowth. It is important to point out that cells derived from pluripotent cells differentiated via conventional *in vitro* methods present no lesser risk. In fact, previous transplantation studies with pluripotent cells modified to overexpress PAX3 and differentiated *in vitro* found that teratomas developed in some recipients when non-mesodermal cells were not eliminated (Darabi et al., 2008). This problem was solved by FACS, sorting the progenitors of interest away from the bulk of differentiating cells. Teratomas have even arisen when porcine fetal tissue was grafted into adult recipients. In these studies, isolated liver, pancreas, and lung, taken from early developmental stages but well after pluripotent cells are thought no longer to be present, generated teratomas when implanted under the kidney capsule (Eventov-Friedman et al., 2005). Therefore, regardless of whether differentiation is performed *in vitro*, *in vivo*, or from fetal donors, cell purification must be equally rigorous to address the risks of teratomagenesis in the recipient, and teratoma differentiation is no more risky than *in vitro* differentiation in this regard. In the current study, no teratomas were observed in any mice transplanted with teratoma-derived α7+ VCAM+ cells and followed for over 12 months. In addition, we found no evidence of abnormally maintained proliferation, as measured by EdU incorporation, in muscle reconstituted from teratoma-derived α7+ VCAM+ cells. The engrafted mononuclear fraction stays quiescent as long as the muscle is not injured. Upon re-injury, however, these cells readily incorporate EdU, proliferate, and generate new fibers, as would be expected from normal quiescent skeletal muscle stem cells.

Differentiation via teratoma provides several advantages. It is technically simple, inexpensive, and capable of producing large quantities of skeletal muscle stem cells. However, its most striking feature is the scale of contribution to tissue regeneration after transplantation. The greatest engraftment previously documented in studies of monolayer *in vitro*-differentiated pluripotent cells has been of less than 200 fibers, and this is in the case of transplanting on the order of 1 million cells. In contrast, myogenic progenitors derived from teratomas produce thousands of fibers, contributing approximately 80% of the regenerated TA muscle fibers and over 50% of the total genomic DNA content of the recipient TA muscle, but with orders of magnitude fewer cells transplanted. This level of engraftment is necessary for meaningful force generation and, therefore, provides a benchmark by which future methods can be compared. In the future, this approach may be useful for the development of novel disease models in which pluripotent cells derived from genetic myopathies are used to reconstitute a functional TA muscle in the mouse, allowing the disease process to be studied *in vivo*. It will be important to determine the extent to which human teratomas differentiate similarly to mouse teratomas and whether they also produce skeletal muscle progenitors with high-level engraftment potential. Although no secondary teratomas were ever observed in this study, caution would demand a highly methodical evaluation of safety before considering the use of *in vivo* differentiation via teratoma to obtain human skeletal muscle stem cells for clinical use. In addition, scalability and efficiency in the human system will need to be addressed robustly. However, taken together, differentiation via teratoma represents an interesting and accessible means of generating cells for skeletal muscle regeneration.

STAR★METHODS

Detailed methods are provided in the online version of this paper and include the following:

- KEY RESOURCES TABLE
- CONTACT FOR REAGENT AND RESOURCE SHARING
- EXPERIMENTAL MODEL AND SUBJECT DETAILS
  - ES and iPS cells culture
  - Irradiated MEFs generation
  - Pax7-ZsGreen reporter iPS cells generation
  - Animals
- MODEL DETAILS
  - Cell transplantation and harvest
  - Cardiotoxin re-injury and EdU administration
  - Functional evaluation on isolated muscles
  - FACS
  - Myogenic differentiation of cultured cells
  - Gene expression analysis
  - SCID PCR
  - Immunostaining on sorted cells
  - Immunostaining on muscle sections
  - Fiber counting and area measurement
  - RNA-seq
- QUANTIFICATION AND STATISTICAL ANALYSIS
  - Software
  - RNA-seq analysis
  - Statistical analysis
- DATA AND SOFTWARE AVAILABILITY

SUPPLEMENTAL INFORMATION

Supplemental Information includes four figures and four tables and can be found with this article online at https://doi.org/10.1016/j.stem.2018.06.010.

A video abstract is available at https://doi.org/10.1016/j.stem.2018.06.010#mmc6.

ACKNOWLEDGMENTS

The authors would like to thank Jinjoo Kang, Olivia Recht, and Cara-Lin Lonetree for their help with genotyping and animal husbandry. The monoclonal antibodies to PAX7, embryonic MHC, MHC, MHC-I, MHC-IIa, and MHC-IIb were obtained from the Developmental Studies Hybridoma Bank developed under the auspices of the NICHD and maintained by the University of Iowa. Plasmids pMXs-Oct3/4, pMXs-Sox2, and pMXs-Klf4 were gifts from Shinya Yamanaka via Addgene. The study was supported by National Institute of Neurological Disorders and Stroke (NINDS) grant R01 NS083549 (to M.K.), National Institute of Arthritis and Musculoskeletal and Skin Diseases (NIAMS) grant R01 AR055299 (to R.C.R.P.), Regenerative Medicine Minnesota discovery science grant RMM 102516 001 (to S.S.-K.C.), and the Greg Marzolf Jr. Foundation (2016.MK).

AUTHOR CONTRIBUTIONS

Conceptualization, M.K.; Methodology, M.K., R.C.R.P., R.W.A., and S.S.-K.C.; Investigation, J.S.P., M.P.P., N.X., R.W.A., and S.S.-K.C.; Formal Analysis, S.S.-K.C.; Resources, A.F. and R.C.R.P.; Writing – Original Draft, M.K. and S.S.-K.C.; Writing – Review & Editing, M.K. and S.S.-K.C.; Visualization, M.K. and S.S.-K.C.; Funding Acquisition, M.K., R.C.R.P., and S.S.-K.C.; Supervision, M.K.

DECLARATION OF INTERESTS

The authors declare no competing interests.

Received: January 11, 2017
Revised: March 14, 2018
Accepted: June 14, 2018
Published: July 5, 2018

REFERENCES

Afgan, E., Baker, D., van den Beek, M., Blankenberg, D., Bouvier, D., Čech, M., Chilton, J., Clements, D., Coraor, N., Eberhard, C., et al. (2016). The Galaxy platform for accessible, reproducible and collaborative biomedical analyses: 2016 update. Nucleic Acids Res. *44* (W1), W3–W10.

Amabile, G., Welner, R.S., Nombela-Arrieta, C., D'Alise, A.M., Di Ruscio, A., Ebralidze, A.K., Kraytsberg, Y., Ye, M., Kocher, O., Neuberg, D.S., et al. (2013). In vivo generation of transplantable human hematopoietic cells from induced pluripotent stem cells. Blood *121*, 1255–1264.

Arpke, R.W., Darabi, R., Mader, T.L., Zhang, Y., Toyama, A., Lonetree, C.L., Nash, N., Lowe, D.A., Perlingeiro, R.C., and Kyba, M. (2013). A new immuno-, dystrophin-deficient model, the NSG-mdx(4Cv) mouse, provides evidence for functional improvement following allogeneic satellite cell transplantation. Stem Cells *31*, 1611–1620.

Blanco-Bose, W.E., Yao, C.C., Kramer, R.H., and Blau, H.M. (2001). Purification of mouse primary myoblasts based on alpha 7 integrin expression. Exp. Cell Res. *265*, 212–220.

Bober, E., Franz, T., Arnold, H.H., Gruss, P., and Tremblay, P. (1994). Pax-3 is required for the development of limb muscles: a possible role for the migration of dermomyotomal muscle progenitor cells. Development *120*, 603–612.

Bosnakovski, D., Xu, Z., Li, W., Thet, S., Cleaver, O., Perlingeiro, R.C., and Kyba, M. (2008). Prospective isolation of skeletal muscle stem cells with a Pax7 reporter. Stem Cells *26*, 3194–3204.

Brack, A.S., Bildsoe, H., and Hughes, S.M. (2005). Evidence that satellite cell decrement contributes to preferential decline in nuclear number from large fibres during murine age-related muscle atrophy. J. Cell Sci. *118*, 4813–4821.

Chal, J., Oginuma, M., Al Tanoury, Z., Gobert, B., Sumara, O., Hick, A., Bousson, F., Zidouni, Y., Mursch, C., Moncuquet, P., et al. (2015). Differentiation of pluripotent stem cells to muscle fiber to model Duchenne muscular dystrophy. Nat. Biotechnol. *33*, 962–969.

Chan, S.S., Shi, X., Toyama, A., Arpke, R.W., Dandapat, A., Iacovino, M., Kang, J., Le, G., Hagen, H.R., Garry, D.J., and Kyba, M. (2013). Mesp1 patterns mesoderm into cardiac, hematopoietic, or skeletal myogenic progenitors in a context-dependent manner. Cell Stem Cell *12*, 587–601.

Collins, C.A., Olsen, I., Zammit, P.S., Heslop, L., Petrie, A., Partridge, T.A., and Morgan, J.E. (2005). Stem cell function, self-renewal, and behavioral heterogeneity of cells from the adult muscle satellite cell niche. Cell *122*, 289–301.

Darabi, R., Gehlbach, K., Bachoo, R.M., Kamath, S., Osawa, M., Kamm, K.E., Kyba, M., and Perlingeiro, R.C. (2008). Functional skeletal muscle regeneration from differentiating embryonic stem cells. Nat. Med. *14*, 134–143.

Darabi, R., Arpke, R.W., Irion, S., Dimos, J.T., Grskovic, M., Kyba, M., and Perlingeiro, R.C. (2012). Human ES- and iPS-derived myogenic progenitors restore DYSTROPHIN and improve contractility upon transplantation in dystrophic mice. Cell Stem Cell *10*, 610–619.

Eventov-Friedman, S., Katchman, H., Shezen, E., Aronovich, A., Tchorsh, D., Dekel, B., Freud, E., and Reisner, Y. (2005). Embryonic pig liver, pancreas, and lung as a source for transplantation: optimal organogenesis without teratoma depends on distinct time windows. Proc. Natl. Acad. Sci. USA *102*, 2928–2933.

Filareto, A., Parker, S., Darabi, R., Borges, L., Iacovino, M., Schaaf, T., Mayerhofer, T., Chamberlain, J.S., Ervasti, J.M., McIvor, R.S., et al. (2013). An ex vivo gene therapy approach to treat muscular dystrophy using inducible pluripotent stem cells. Nat. Commun. *4*, 1549.

Fukada, S., Uezumi, A., Ikemoto, M., Masuda, S., Segawa, M., Tanimura, N., Yamamoto, H., Miyagoe-Suzuki, Y., and Takeda, S. (2007). Molecular signature of quiescent satellite cells in adult skeletal muscle. Stem Cells *25*, 2448–2459.

Goulding, M., Lumsden, A., and Paquette, A.J. (1994). Regulation of Pax-3 expression in the dermomyotome and its role in muscle development. Development *120*, 957–971.

Günther, S., Kim, J., Kostin, S., Lepper, C., Fan, C.M., and Braun, T. (2013). Myf5-positive satellite cells contribute to Pax7-dependent long-term maintenance of adult muscle stem cells. Cell Stem Cell *13*, 590–601.

Gussoni, E., Pavlath, G.K., Lanctot, A.M., Sharma, K.R., Miller, R.G., Steinman, L., and Blau, H.M. (1992). Normal dystrophin transcripts detected in Duchenne muscular dystrophy patients after myoblast transplantation. Nature *356*, 435–438.

Hall, J.K., Banks, G.B., Chamberlain, J.S., and Olwin, B.B. (2010). Prevention of muscle aging by myofiber-associated satellite cell transplantation. Sci. Transl. Med. *2*, 57ra83.

Huang, W., Sherman, B.T., and Lempicki, R.A. (2009a). Bioinformatics enrichment tools: paths toward the comprehensive functional analysis of large gene lists. Nucleic Acids Res. *37*, 1–13.

Huang, W., Sherman, B.T., and Lempicki, R.A. (2009b). Systematic and integrative analysis of large gene lists using DAVID bioinformatics resources. Nat. Protoc. *4*, 44–57.

Ismailoglu, I., Yeamans, G., Daley, G.Q., Perlingeiro, R.C., and Kyba, M. (2008). Mesodermal patterning activity of SCL. Exp. Hematol. *36*, 1593–1603.

Jesse, T.L., LaChance, R., Iademarco, M.F., and Dean, D.C. (1998). Interferon regulatory factor-2 is a transcriptional activator in muscle where It regulates expression of vascular cell adhesion molecule-1. J. Cell Biol. *140*, 1265–1276.

Kim, D., Pertea, G., Trapnell, C., Pimentel, H., Kelley, R., and Salzberg, S.L. (2013). TopHat2: accurate alignment of transcriptomes in the presence of insertions, deletions and gene fusions. Genome Biol. *14*, R36.

Kuang, S., Chargé, S.B., Seale, P., Huh, M., and Rudnicki, M.A. (2006). Distinct roles for Pax7 and Pax3 in adult regenerative myogenesis. J. Cell Biol. *172*, 103–113.

Kyba, M., Perlingeiro, R.C., and Daley, G.Q. (2002). HoxB4 confers definitive lymphoid-myeloid engraftment potential on embryonic stem cell and yolk sac hematopoietic progenitors. Cell *109*, 29–37.

Mauro, A. (1961). Satellite cell of skeletal muscle fibers. J. Biophys. Biochem. Cytol. *9*, 493–495.

Mendell, J.R., Kissel, J.T., Amato, A.A., King, W., Signore, L., Prior, T.W., Sahenk, Z., Benson, S., McAndrew, P.E., Rice, R., et al. (1995). Myoblast transfer in the treatment of Duchenne's muscular dystrophy. N. Engl. J. Med. *333*, 832–838.

Montarras, D., Morgan, J., Collins, C., Relaix, F., Zaffran, S., Cumano, A., Partridge, T., and Buckingham, M. (2005). Direct isolation of satellite cells for skeletal muscle regeneration. Science *309*, 2064–2067.

Partridge, T.A., Morgan, J.E., Coulton, G.R., Hoffman, E.P., and Kunkel, L.M. (1989). Conversion of mdx myofibres from dystrophin-negative to -positive by injection of normal myoblasts. Nature *337*, 176–179.

Penton, C.M., Badarinarayana, V., Prisco, J., Powers, E., Pincus, M., Allen, R.E., and August, P.R. (2016). Laminin 521 maintains differentiation potential of mouse and human satellite cell-derived myoblasts during long-term culture expansion. Skelet. Muscle *6*, 44.

Perlingeiro, R.C., Kyba, M., and Daley, G.Q. (2001). Clonal analysis of differentiating embryonic stem cells reveals a hematopoietic progenitor with primitive erythroid and adult lymphoid-myeloid potential. Development *128*, 4597–4604.

Sacco, A., Doyonnas, R., Kraft, P., Vitorovic, S., and Blau, H.M. (2008). Self-renewal and expansion of single transplanted muscle stem cells. Nature *456*, 502–506.

Seale, P., Sabourin, L.A., Girgis-Gabardo, A., Mansouri, A., Gruss, P., and Rudnicki, M.A. (2000). Pax7 is required for the specification of myogenic satellite cells. Cell *102*, 777–786.

Seale, P., Ishibashi, J., Holterman, C., and Rudnicki, M.A. (2004). Muscle satellite cell-specific genes identified by genetic profiling of MyoD-deficient myogenic cell. Dev. Biol. *275*, 287–300.

Shelton, M., Metz, J., Liu, J., Carpenedo, R.L., Demers, S.P., Stanford, W.L., and Skerjanc, I.S. (2014). Derivation and expansion of PAX7-positive muscle progenitors from human and mouse embryonic stem cells. Stem Cell Reports *3*, 516–529.

Suzuki, N., Yamazaki, S., Yamaguchi, T., Okabe, M., Masaki, H., Takaki, S., Otsu, M., and Nakauchi, H. (2013). Generation of engraftable hematopoietic stem cells from induced pluripotent stem cells by way of teratoma formation. Mol. Ther. *21*, 1424–1431.

Takahashi, K., and Yamanaka, S. (2006). Induction of pluripotent stem cells from mouse embryonic and adult fibroblast cultures by defined factors. Cell *126*, 663–676.

Trapnell, C., Williams, B.A., Pertea, G., Mortazavi, A., Kwan, G., van Baren, M.J., Salzberg, S.L., Wold, B.J., and Pachter, L. (2010). Transcript assembly and quantification by RNA-Seq reveals unannotated transcripts and isoform switching during cell differentiation. Nat. Biotechnol. *28*, 511–515.

von Maltzahn, J., Jones, A.E., Parks, R.J., and Rudnicki, M.A. (2013). Pax7 is critical for the normal function of satellite cells in adult skeletal muscle. Proc. Natl. Acad. Sci. USA *110*, 16474–16479.

STAR★METHODS

KEY RESOURCES TABLE

REAGENT or RESOURCE	SOURCE	IDENTIFIER
Antibodies		
APC α7-Integrin	AbLab	Cat#67-0010-05
Alexa Fluor 555 α-Bungarotoxin	Invitrogen	Cat#B35451; RRID:AB_2617152
APC β1-Integrin (CD29)	eBioscience	Cat#17-0291-82; RRID:AB_1210793
PE-Cy7 CD31 (PECAM)	BD Biosciences	Cat#561410; RRID:AB_10612003
Biotin CD34	eBioscience	Cat#13-0341-81; RRID:AB_466424
PE-Cy7 CD45	BD Biosciences	Cat#552848; RRID:AB_394489
Biotin CXCR4	eBioscience	Cat#13-9991-82; RRID:AB_10609202
DYSTROPHIN	Abcam	Cat#ab15277; RRID:AB_301813
EGFP	Abcam	Cat#ab13970; RRID:AB_300798
Embryonic myosin heavy chain	Developmental Studies Hybridoma Bank	Cat#F1.652; RRID:AB_528358
Laminin	Sigma	Cat#L9393; RRID:AB_477163
MHC-I	Developmental Studies Hybridoma Bank	Cat#BA-D5; RRID:AB_2235587
MHC-IIa	Developmental Studies Hybridoma Bank	Cat#SC-71; RRID:AB_2147165
MHC-IIb	Developmental Studies Hybridoma Bank	Cat#BF-F3; RRID:AB_2266724
MYOD1	Santa Cruz Biotechnology	Cat#sc-304; RRID:AB_631992
PAX7	Developmental Studies Hybridoma Bank	Cat#PAX7; RRID:AB_528428
Sarcomeric MHC	Developmental Studies Hybridoma Bank	Cat#MF-20; RRID:AB_2147781
Biotin VCAM-1	BD Biosciences	Cat#553331; RRID:AB_394787
Streptavidin-PE	BD Biosciences	Cat#554061; RRID:AB_10053328
Chemicals, Peptides, and Recombinant Proteins		
KO-DMEM	Life Technologies	Cat#10829-018
DMEM, high glucose	HyClone	Cat#SH30081.01
DMEM/F12	Cellgro	Cat#15-090-CV
FBS	PEAK serum	Cat#PS-FBS
ESC-qualified FBS	Gemini Bio-Products	Cat#100-119
Horse serum	HyClone	Cat#SH30074.03
Non-essential amino acids	Life Technologies	Cat#11140-050
Penicillin/streptomycin	Life Technologies	Cat#15140-122
Glutamax	Millipore	Cat#SCR006
β-Mercaptoethanol	Sigma	Cat#M3148
Leukemia inhibitory factor	Millipore	Cat#ESG1107
Chick embryo extract	US Biological	Cat#C3999
Insulin-transferrin-selenium	Life Technologies	Cat#41400045
Basic FGF	R&D Systems	Cat#233-FB/CF
Propidium iodide	Sigma	Cat#P4170
Paraformaldehyde	Sigma	Cat#P6148
Triton X-100	Sigma	Cat#X100
Bovine serum albumin	Fisher Bioreagents	Cat#BP1605-100
PBS	HyClone	Cat#SH30256.01
Gelatin	Sigma	Cat#G2500
0.25% Trypsin-EDTA	Life Technologies	Cat#25200-072
DAPI	Life Technologies	Cat#D3571
OCT solution	Scigen	Cat#4586
2-Methylbutane	Sigma	Cat#320404

(*Continued on next page*)

Continued

REAGENT or RESOURCE	SOURCE	IDENTIFIER
Acetone	Sigma	Cat#179124
DAKO Retrieval Solution	Agilent	Cat#S169984-2
Immu-Mount	Thermo Scientific	Cat#9990402
Cardiotoxin	Sigma-Aldrich	Cat#C9759
Ketamine (VetaKet)	Akorn	NDC:59399-114-10
Xylazine (AnaSed)	Akorn	NDC:59399-111-50
Avertin (tribromoethanol)	Sigma	Cat#T48402
EdU	Invitrogen	Cat#A10044
NaCl	Fisher Bioreagents	Cat#BP358-212
$NaHCO_3$	Sigma	Cat#S7277
Glucose	Sigma	Cat#G7021
KCl	Fisher Bioreagents	Cat#BP366-500
$CaCl_2$	Sigma	Cat#21097
$MgSO_4$	Sigma	Cat#M7506
NaH_2PO_4	Sigma	Cat#S8282
Sodium pyruvate	Sigma	Cat#P5280
GoTaq Flexi DNA polymerase	Promega	Cat#M8298
Premix Ex Taq (probe qPCR) master mix	Clontech	Cat#RR39WR
AluI	New England BioLabs	Cat#R0137S
Critical Commercial Assays		
RNeasy Mini Kit	QIAGEN	Cat#74106
Verso cDNA Synthesis Kit	Thermo Scientific	Cat#AB1453A
SMARTer Stranded Total RNA-Seq Kit – Pico Input Mammalian Kit	Clontech	Cat#634411
Click-iT EdU Alexa Fluor 555 Imaging Kit	Invitrogen	Cat#C10338
GeneJET Genomic DNA Purification Kit	Thermo Scientific	Cat#K0721
Deposited Data		
RNA-seq	This paper	GEO: GSE92892
ES-Bruce4 RNA-seq	https://www.encodeproject.org/	GEO: GSE93453
Hematopoietic multipotent progenitor cell RNA-seq	https://www.encodeproject.org/	GEO: GSE90209
Experimental Models: Cell Lines		
Mouse embryonic fibroblasts	This paper	N/A
E14-EGFP mouse ESCs	Ismailoglu et al., 2008	N/A
C57BL/6N-PRX-B6N #1 mouse ESCs	The Jackson Laboratory (via Mouse Genetics Laboratory, University of Minnesota)	Stock#012448
Pax7-ZsGreen mouse iPS cells	This paper	N/A
Experimental Models: Organisms/Strains		
NSG-mdx^{4Cv} mice	Arpke et al., 2013	N/A
Pax7-ZsGreen mice	Bosnakovski et al., 2008	N/A
129P2/OlaHsd mice	Envigo	N/A
Oligonucleotides		
Taqman qPCR assay: *Gapdh*	Applied Biosystems	Mm99999915_g1
Taqman qPCR assay: *Myf5*	Applied Biosystems	Mm00435125_m1
Taqman qPCR assay: *Myod1*	Applied Biosystems	Mm00440387_m1
Taqman qPCR assay: *Pax3*	Applied Biosystems	Mm00435491_m1
Taqman qPCR assay: *Pax7*	Applied Biosystems	Mm00834079_m1

(*Continued on next page*)

Continued		
REAGENT or RESOURCE	SOURCE	IDENTIFIER
SCID PCR forward primer	GGA AAA GAA TTG GTA TCC AC	N/A
SCID PCR reverse primer	AGT TAT AAC AGC TGG GTT GGC	N/A
Recombinant DNA		
pMXs-Oct3/4	Addgene	Plasmid#13366
pMXs-Sox2	Addgene	Plasmid#13367
pMXs-Klf4	Addgene	Plasmid#13370
Software and Algorithms		
ImageJ (v2.0.0-rc-65/1.52a)	NIH	https://imagej.nih.gov/ij/
FlowJo (v7.6.3)	FLOWJO LLC	https://www.flowjo.com/
Prism (v6.07)	GraphPad Software	https://www.graphpad.com/scientific-software/prism/
ZEN (v2.3 pro)	Zeiss	https://www.zeiss.com/
LabChart (v6.1.1)	ADInstruments	https://www.adinstruments.com/products/labchart/
FACSDiva (v6.1.3)	BD Biosciences	http://www.bdbiosciences.com/
Adobe Photoshop CS3 Extended (v10.0)	Adobe	https://www.adobe.com/products/photoshop.html

CONTACT FOR REAGENT AND RESOURCE SHARING

Further information and requests for resources and reagents should be directed to and will be fulfilled by the Lead Contact, Michael Kyba (kyba@umn.edu).

EXPERIMENTAL MODEL AND SUBJECT DETAILS

ES and iPS cells culture

E14-EGFP male mouse ES cells (Ismailoglu et al., 2008), C57BL/6N-PRX-B6N #1 male mouse ES cells (The Jackson Laboratory #012448, Bar Harbor, ME, via Mouse Genetics Laboratory, University of Minnesota) and *Pax7*-ZsGreen reporter mouse iPS cells were cultured on irradiated mouse embryonic fibroblasts (MEFs) in maintenance medium consisting of: Knock-Out Dulbecco's Minimum Essential Medium (KO-DMEM) (Life Technologies #10829-018, Grand Island, NY), 15% ES cells-qualified fetal bovine serum (ES-FBS) (Gemini Bio-Products #100-119, West Sacramento, CA), 1% non-essential amino acids (NEAA) (Life Technologies #11140-050), 1% penicillin/streptomycin (P/S) (Life Technologies #15140-122), 2 mM Glutamax (Life Technologies #SCR006), 0.1 mM β-mercaptoethanol (Sigma #M3148, St. Louis, MO) and 500 U/ml leukemia inhibitory factor (Millipore #ESG1107, Temecula, CA), at 37°C in 5% CO_2. On the day of transplantation for generating teratomas, ES and iPS cells were trypsinized and plated on a tissue culture flask for 45-60 min to remove MEFs.

Irradiated MEFs generation

MEFs were harvested from E14.5 embryos. After removing the head and the internal organs, the remaining parts were minced into little pieces and digested with 0.25% trypsin-EDTA (Life Technologies #25200-072) for 20 min at 37°C. Cells from 3-4 embryos were pooled and cultured in a T75 flask in DMEM (HyClone #SH30081.01, Logan, UT) with 10% FBS (PEAK serum #PS-FBS, Wellington, CO) and 2 mM Glutamax at 37°C in 5% CO_2. Cells were passaged at 1:4-1:5 when confluent. By passage 4, cells were irradiated with 5000 cGy using a RS 2000 Biological Research Irradiator (Rad Source Technologies, Suwanee, GA) to generate irradiated MEFs.

Pax7-ZsGreen reporter iPS cells generation

For iPS cell generation, fibroblasts cultures were established by trypsin digestion of tail-tip biopsies taken from 3 week-old *Pax7*-ZsGreen male mice (Bosnakovski et al., 2008). Tail tip fibroblasts were seeded on irradiated MEFs in DMEM with 10% FBS and infected with Oct4 (Addgene #13366), Sox2 (Addgene #13367) and Klf4 (Addgene #13370) retroviruses (gifts from Shinya Yamanaka via Addgene, Cambridge, MA) (Takahashi and Yamanaka, 2006). Twenty-four hours after transduction, medium was switched to ES cell maintenance medium, and 2–3 weeks later, iPS colonies were individually isolated (Filareto et al., 2013).

Animals

Housing, husbandry and all procedures involving animals used in this study were performed in compliance with protocols (#1408-31770A, #1708-35046A) approved by the University of Minnesota Institutional Animal Care and Use Committee and under institutional assurances of AAALAC accreditation (#000552, as of Nov 2015), USDA research facility registration (USDA No. 41-R-0005),

and PHS Animal Welfare Assurance approval (A3456-01). Mice were group housed (up to 4 animals per cage for males and 5 for females) on a 12:12 hr light-dark cycle, with free access to food and water in individually ventilated specific pathogen free (SPF) cages. All mice used were healthy and were not involved in any previous procedures nor drug treatment unless indicated otherwise. NSG-mdx^{4Cv} mice were generated by crossing NOD.Cg-*Prkdc*^{scid}*Il2rg*^{tm1Wjl}/SzJ (NSG) mice and B6Ros.Cg-*Dmd*$^{mdx\text{-}4Cv}$/J (mdx^{4Cv}) mice, as previously reported (Arpke et al., 2013) and maintained in autoclaved cages. For teratoma formation and cell transplantation, 3–4 month-old homozygous NSG-mdx^{4Cv} mice from both sexes were randomly allocated to experimental groups. Our preliminary results do not suggest any sex influence on the study outcomes. *Pax7*-ZsGreen mice, from which *Pax7*-ZsGreen reporter iPS cells derive, were generated by pronuclear injection of a mouse *Pax7* locus-containing BAC with exon 1 of *Pax7* coding sequence replaced by a ZsGreen coding sequence, as previously reported (Bosnakovski et al., 2008). *Pax7*-ZsGreen mice used were heterozygous in a C57BL/6 × 129P2/OlaHsd hybrid background. Wild-type 129P2/OlaHsd mice were obtained from Envigo (Indianapolis, IN).

MODEL DETAILS

Cell transplantation and harvest

Recipient NSG-mdx^{4Cv} mice (3–4 month-old) were anesthetized with ketamine (150 mg/kg, i.p., Akorn NDC:59399-114-10, Lake Forest, IL) and xylazine (10 mg/kg, i.p., Akorn NDC:59399-111-50), and both hindlimbs were irradiated with 1200 cGy, two days prior to intramuscular injection of cells. A lead shield permitted exposure only to the hindlimbs. One day prior to transplantation, cardiotoxin (10 μM in 15 μl, Sigma #C9759) was injected into both left and right TA muscles of each mouse to induce muscle injury. For teratoma induction, 250,000 ES cells or 1,000,000 iPS cells were resuspended in 10 μL sterile PBS (HyClone #SH30256.01) and injected using a Hamilton syringe (Hamilton, Reno, NV). For transplantation of myogenic progenitors, sorted α7+ VCAM+ cells (40,000, 20,000 and 20,000 cells from E14 ES cell-, C57BL/6N ES cells- and iPS cell-derived teratomas respectively, and 900 cells from transplanted TAs) were injected into the left TA while PBS was injected into the right TA. TAs were harvested at 3–4 weeks (for teratomas) or 1–12 months (for myogenic progenitors) after transplantation and were analyzed by FACS or immunohistochemistry.

Cardiotoxin re-injury and EdU administration

Transplanted TA muscles were re-injured with cardiotoxin (10 μM in 15 μl) injections 3 months after the primary transplant. Two days later, EdU (5-ethynyl-2′-deoxyuridine) (Invitrogen #A10044, Carlsbad, CA) was administered intraperitoneally (0.1 mg/20 g body weight) twice a day for 3 days. Muscles were harvested 5 days or 5 weeks after injury.

Functional evaluation on isolated muscles

Mice were anesthetized with Avertin (250 mg/kg, i.p., Sigma #T48402) and TA muscles were isolated and connected to a force transducer (model #FT03, Grass Instrument, West Warwick, RI) in the Radnoti 4 Chamber Tissue-Organ Bath apparatus (ADInstruments, Colorado Springs, CO). Isolated tissues were bathed in Ringer solution (120.5 mM NaCl (Fisher Bioreagents #BP358-212, Pittsburgh, PA), 20.4 mM $NaHCO_3$ (Sigma #S7277), 10 mM glucose (Sigma #G7021), 4.8 mM KCl (Fisher Bioreagents #BP366-500), 1.6 mM $CaCl_2$ (Sigma #21097), 1.2 mM $MgSO_4$ (Sigma #M7506), 1.2 mM NaH_2PO_4 (Sigma #S8282), 1.0 mM sodium pyruvate (Sigma #P5280), adjusted to pH 7.4) at 25°C with 95% O_2/5% CO_2 perfusion. A pair of platinum electrodes was placed longitudinally on either side of the muscles for electrical stimulation using square wave pulses at 25 V, 0.2 ms duration and 150 Hz. Muscles were maintained at optimum length (L_0), which was empirically determined to generate the maximal tetanic force (F_0) upon stimulation. Fatigue time was defined as the time required for force to drop to 30% of F_0 after 1-min pulse of stimulation. Total muscle cross-sectional area (CSA) was calculated by dividing muscle mass by the product of muscle length and muscle density (1.06 mg/mm^3). Specific force (sF_0) was subsequently calculated by normalizing F_0 to CSA. Data acquisition was performed in a PowerLab 8/30 using the LabChart software (both ADInstruments).

FACS

Dissociated cells were incubated with antibodies (APC anti-α7-Integrin, AbLab #67-0010-05, Vancouver, Canada; APC anti-β1-Integrin, eBioscience #17-0291-82; RRID:AB_1210793, San Diego, CA; PE-Cy7 anti-CD31, BD Biosciences Cat#561410; RRID:AB_10612003, San Jose, CA; Biotin anti-CD34, eBioscience Cat#13-0341-81; RRID:AB_466424; PE-Cy7 anti-CD45, BD Biosciences Cat#552848; RRID:AB_394489; Biotin anti-CXCR4, eBioscience Cat#13-9991-82; RRID:AB_10609202; Biotin anti-VCAM-1, BD Biosciences Cat#553331; RRID:AB_10053328; PE streptavidin, BD Biosciences Cat#554061; all at 0.5 μL per 1 million cells) on ice for 30 min. Propidium iodide (PI) (1 μg/ml, Sigma #P4170) was added to differentiate between live and dead cells. Only live cells (PI–) were counted. FACS analysis and cell sorting were performed in a BD FACSAriaII (BD Biosciences, San Diego, CA) using the FACSDiva software (BD Biosciences). Single-cell precision was used for sorting single cells into 96-well plate for clonal analysis, and 4-way purity precision was used for bulk sort. Data were analyzed using FlowJo (FLOWJO LLC, Ashland, OR). Further information on antibodies used is listed in Key Resources Table.

Myogenic differentiation of cultured cells

To access *in vitro* myogenic potential of various cell fractions or single cells, FACS-sorted cells were cultured in myogenic medium: DMEM/F12 (Cellgro #15-090-CV, Manassas, VA), 20% FBS, 10% horse serum (HyClone #SH30074.03), 10 ng/ml basic FGF (R&D Systems #233-FB/CF, Minneapolis, MN), 1% P/S, 2 mM Glutamax and 0.5% chick embryo extract (US Biological #C3999, Salem,

MA). After 8 days in culture, cells were analyzed for MHC positivity by immunostaining. For long-term expansion experiments, cells were cultured in myogenic expansion medium: DMEM/F12, 20% FBS, 10 ng/ml basic FGF, 1% P/S, 2 mM Glutamax and 0.1 mM β-mercaptoethanol, and passaged every 7 days. To assess myotube formation, cells were switched to myogenic differentiation medium: high-glucose DMEM, 2% horse serum, 1% insulin-transferrin-selenium (Life Technologies #41400045) and 1% P/S for 3 days, and followed by immunostaining.

Gene expression analysis

Total RNA was extracted using RNeasy Mini Kit (QIAGEN #74106, Valencia, CA), and subsequent genomic DNA removal and reverse transcription (RT) were performed using Verso cDNA Synthesis Kit (Thermo Scientific #AB1453A, Pittsburgh, PA). Quantitative reverse transcription polymerase chain reaction (qRT-PCR) was performed in triplicate using Taqman probes (Applied Biosystems, Carlsbad, CA) and Premix Ex Taq (probe qPCR) master mix (Clontech #RR39WR, Mountain View, CA). Expression of individual genes was subsequently analyzed by the ΔCt method in relative to the expression of the housekeeping gene *Gapdh* in a QuantStudio 6 Flex Real-Time PCR System using QuantStudio Real-Time PCR Software (both Applied Biosystems).

SCID PCR

Genomic DNA was extracted using the GeneJet Genomic DNA Purification kit (Thermo Scientific #K0721). DNA was amplified by GoTaq Flexi DNA polymerase (Promega #M8298, Madison, WI) using the following primers: forward: GGA AAA GAA TTG GTA TCC AC, reverse: AGT TAT AAC AGC TGG GTT GGC. PCR product was then digested by AluI (New England BioLabs #R0137S, Ipswich, MA) and analyzed in an 8% polyacrylamide gel.

Immunostaining on sorted cells

Cells were fixed with 4% paraformaldehyde (PFA) (Sigma #P6148) for 60 min, permeabilized with 0.3% Triton X-100 (Sigma #X100) for 30 min, and blocked with 3% bovine serum albumin (BSA) (Fisher Bioreagents #BP1605-100) for 1 hr, all at room temperature. Primary antibodies (anti-DYSTROPHIN at 1:250, Abcam Cat#ab15277; RRID:AB_301813, Cambridge, UK; anti-MHC at 1:20, Developmental Studies Hybridoma Bank (DSHB) Cat#MF-20; RRID:AB_2147781, Iowa City, IA; anti-MYOD1 at 1:100, Santa Cruz Biotechnology Cat#sc-304; RRID:AB_631992, Dallas, TX; and anti-PAX7 at 1:100, DSHB Cat#PAX7; RRID:AB_528428) were incubated overnight at 4°C followed by Alexa Fluor-448, −555 or −647 conjugated secondary antibodies (Life Technologies) for 60 min at room temperature. Cells were counterstained with 4',6-diamidino-2-phenylindole (DAPI) (Life Technologies #D3571). For cytospins, dissociated cells were spun onto coverslips via cytology funnels (Biomedical Polymers, Gardner, MA), and were air-dried for at least 1 hr before subsequent fixation and immunostaining as described above. Images were acquired with a Zeiss Axio Imager M1 upright microscope with an AxioCam HRc camera using the ZEN software (Zeiss). Further information on antibodies used is listed in Key Resources Table.

Immunostaining on muscle sections

TA muscles were harvested and embedded with optimal cutting temperature (OCT) solution (Scigen #4586, Gardena, CA) and snap frozen with liquid nitrogen-cooled 2-methylbutane (Sigma #320404). For EGFP staining, TA muscles were prefixed with 4% PFA overnight at 4°C following by a 20%/30% sucrose gradient treatment before embedding. Tissues were sectioned at 10 μm with a Leica CM3050 S cryostat (Leica Microsystems, Buffalo Grove, IL). For DYSTROPHIN staining, sections were fixed with ice-cold acetone (Sigma #179124) for 5 min. For PAX7 staining, sections were fixed with 4% PFA for 10 min, following by antigen retrieval with DAKO Retrieval Solution (Agilent #S169984-2, Santa Clara, CA) at 95°C for 20 min. Subsequent immunostaining procedures were identical to those of sorted cells as described above, except that coverslips were mounted with Immu-Mount (Thermo Scientific #9990402) before imaging. Primary antibodies used are Alexa Fluor 555 anti-α-bungarotoxin (1:100, Invitrogen Cat#B35451; RRID:AB_2617152), anti-DYSTROPHIN (1:250, Abcam Cat#ab15277; RRID:AB_301813), anti-EGFP (1:500, Abcam Cat#ab13970; RRID:AB_300798), anti-embryonic MHC (1:20, DSHB Cat#F1.652; RRID:AB_528358), anti-laminin (1:500, Sigma Cat#L9393; RRID:AB_477163), anti-MHC-I (1:100, DSHB Cat#BA-D5; RRID:AB_2235587), anti-MHC-IIa (1:100, DSHB Cat#SC-71; RRID:AB_2147165), anti-MHC-IIb (1:100, DSHB Cat#BF-F3; RRID:AB_2266724), and anti-PAX7 (1:10, DSHB Cat#PAX7; RRID:AB_528428). Further information on antibodies used is listed in Key Resources Table.

Fiber counting and area measurement

Fiber counting and cross section area measurement were performed using ImageJ with the colocalization plugin (NIH). DYSTROPHIN or laminin staining was used to define the cross section area of muscle fibers.

RNA-seq

α7+ VCAM+ cells were FACS-sorted from E14 ES cell teratomas, transplanted TA muscles, and from E14.5 embryos and 8-week-old adult hind limbs from 129P2/OlaHsd mice (Envigo, Indianapolis, IN). Total RNA was extracted with in-column genomic DNA removal using RNeasy Mini Kit, and of which 10 ng was used for sequencing libraries creation using SMARTer Stranded Total RNA-Seq Kit – Pico Input Mammalian Kit (Clontech #634411). Paired-end 50 base-pair sequencing was performed using an Illumina HiSeq2500 (Illumina, San Diego, CA), producing 4–8 million raw reads per sample.

QUANTIFICATION AND STATISTICAL ANALYSIS

Software

FACS data acquisition were performed in FACSDiva v6.1.3 (BD) and analyzed in FlowJo v7.6.3 (FLOWJO LLC). Quantitative PCR data acquisition were performed in QuantStudio Real-Time PCR Software v1.3 (Applied Biosystems). Force measurements were acquired using LabChart v6.1.1 (ADInstruments). Immunostaining data were acquired using ZEN v2.3 pro (Zeiss). Fiber counting and measurements were performed with ImageJ v2.0.0-rc-65/1.52a (NIH). Whole muscle section was composed in Adobe Photoshop CS3 Extended v10.0 (Adobe).

RNA-seq analysis

RNA-seq reads were processed in Galaxy via Minnesota Supercomputing Institute, University of Minnesota (Afgan et al., 2016) with TopHat (Galaxy v2.1.0) (Kim et al., 2013) and Cufflinks (Galaxy v2.2.1.0) (Trapnell et al., 2010) for transcriptome mapping and alignment against the *Mus musculus* genome (mm10). Undifferentiated mouse ES cell RNA-seq dataset and mouse hematopoietic multipotent progenitor cell dataset were obtained from GEO: GSE93453 and GEO: GSE90209 respectively via ENCODE (https://www.encodeproject.org/). Further analysis including hierarchy clustering and differential genes determination was performed using Partek Genomic Suite v6.0 using default parameters (Partek, St. Louis, MI). Significant difference was set with a false discovery rate-adjusted p value < 0.05 and an absolute fold change > 2.5. Gene Ontology (GO) analysis was performed using DAVID Bioinformatics Resources (Huang et al., 2009a, 2009b). RNA-seq datasets can be accessed on GEO: GSE92892.

Statistical analysis

Data are expressed as mean ± SEM. Graphs and statistics are prepared with Prism v6.07 (GraphPad Software, La Jolla, CA). Dose-response relationship is modeled using a log-linear regression model with variable slope. The number of replicates for individual experiments is indicated in the corresponding figure legend. Statistical significance is determined by Student's t test for comparison between two treatment groups, or one-way analysis of variance (ANOVA) with Tukey post hoc test for comparison among three or more treatment groups. Statistical significance is set as $p < 0.05$.

DATA AND SOFTWARE AVAILABILITY

The accession number for the RNA-seq datasets reported in this paper is GEO: GSE92892. Whole muscle section was composed by stitching separate images together using the function Photomerge with the option Interactive Layout in Adobe Photoshop.